

smaller than the scatter in Fig. 4. The drive voltage is monitored continuously and is observed to give a signature at  $T_c$  whose sharpness is consistent with the  $Q$  of the viscometer, ensuring that the temperature is homogenous to within the precision of the measurement.

The  $B$ -phase normal-fluid density data, shown in Fig. 2(b), have been fitted by a function of the form  $\rho_n/\rho = 1 - C(1-t) - D(1-t)^2$ , for  $t > 0.9$ . The coefficients  $C$  and  $D$  are listed in Table I. No significant pressure dependence is seen in the coefficient of the linear term.

The authors would like to acknowledge the assistance of Professor R. A. Buhrman with the SQUID thermometry, and the help of Dr. E. N. Smith with the construction of the Andronikashvili cell.

This work has been supported by the National Science Foundation through Grants No. DMR 75-08624 and No. DMR 76-21669 and by the National Science Foundation through the Cornell Materials Science Center Grant No. DMR 76-01281, MSC Report No. 2951.

<sup>(a)</sup>Present address: Physics Department, Schuster Laboratory, The University of Manchester, Manchester M13 9PL, England.

<sup>(b)</sup>Present address: Bell Laboratories, Murray Hill, N. J. 07974.

<sup>1</sup>T. A. Alvesalo, H. K. Collan, M. T. Laponen, and M. C. Veuro, *Phys. Rev. Lett.* **32**, 981 (1974); T. A. Alvesalo, H. K. Collan, M. T. Laponen, O. V. Lounasmaa, and M. C. Veuro, *J. Low Temp. Phys.* **19**, 1 (1975).

<sup>2</sup>C. J. Pethick, H. Smith, and P. Bhattacharyya, *Phys. Rev. Lett.* **34**, 643 (1975); P. Bhattacharyya, C. J. Pethick, and H. Smith, *Phys. Rev. B* **15**, 3367 (1977).

<sup>3</sup>Y. A. Ono, J. Hara, K. Nagai, and K. Kawamura, *J. Low Temp. Phys.* **27**, 513 (1977).

<sup>4</sup>P. Wölfle, to be published.

<sup>5</sup>P. C. Main, C. W. Kiewiet, W. T. Band, J. R. Hook, D. J. Sandiford, and H. E. Hall, *J. Phys. C* **9**, L397 (1976).

<sup>6</sup>R. W. Guernsey, J. R. McCoy, M. Steinback, and J. K. Lyden, *Phys. Lett.* **58A**, 26 (1976).

<sup>7</sup>J. E. Berthold, R. W. Giannetta, E. N. Smith, and J. D. Reppy, *Phys. Rev. Lett.* **37**, 1138 (1976).

<sup>8</sup>J. C. Wheatley, *Rev. Mod. Phys.* **47**, 415 (1975).

<sup>9</sup>V. J. Emery, *J. Low Temp. Phys.* **22**, 467 (1976).

## Role of Intrinsic Plasmons in Conduction-Band X-Ray Photoemission from Solids

David R. Penn

*National Bureau of Standards, Washington, D. C. 20234*

(Received 14 November 1977; revised manuscript received 7 December 1977)

I show that intrinsic plasmons are created in x-ray photoemission experiments on the conduction bands of simple metals. Unlike the core case, the plasmons are produced by many-body effects and are a direct consequence of electron correlation. A theory of the intrinsic plasmon production is given and a calculation of the electron energy-loss spectra in conduction-band x-ray photoemission from Mg and Na is presented. The calculation takes into account both intrinsic and extrinsic plasmon production and the agreement with experiment is good.

In recent years x-ray photoemission spectroscopy (XPS) from the conduction bands of metals has become an important tool in the determination of electronic densities of states. The purpose of this Letter is to show that intrinsic plasmons are created in XPS experiments on the conduction bands of simple metals and that they play an important role in the XPS loss spectra, i.e., in the plasmon satellites. A theory of intrinsic plasmon creation is presented which shows that the physics of the process is new and quite different from the case of intrinsic plasmon production in core-level XPS. The XPS loss spectra provide the most direct experimental evidence for intrinsic plasmon production and calculations for Mg

and Na are reported and compared to experiment. The contributions of intrinsic plasmons to the first loss peak are estimated to be  $\approx 37\%$  and  $44\%$  in Mg and Na, respectively.

In the case of XPS from the core levels of nearly-free-electron metals a typical loss spectrum consists of several peaks centered at  $E_0$ ,  $E_0 - \hbar\omega_p$ ,  $E_0 - 2\hbar\omega_p$ , etc., where  $\hbar\omega_p$  is the plasma energy. The peaks represent electrons that have excited zero, one, two, etc., plasmons prior to escaping from the solid. Almost ten years ago Lundqvist<sup>1</sup> suggested that a large fraction of the loss spectra was due to intrinsic plasmon production, a process in which the core electron is photoexcited and simultaneously one or more plasmons are

created by the sudden appearance of the core hole potential. In a recent Letter<sup>2</sup> I have demonstrated the importance of intrinsic plasmons in core-level XPS via a quantitative calculation which drew on previous theoretical work,<sup>3,4</sup> and the role of intrinsic plasmons in core-level XPS is fairly well understood at present.

In core-level XPS intrinsic plasmons are produced by the sudden appearance of a localized hole potential. Their production in conduction-band XPS has been overlooked, at least in part because the hole created by the photoexcitation of a conduction electron is delocalized and the potential due to this type of hole does not produce intrinsic plasmons. Nevertheless, the electron-electron interaction allows simultaneous photoexcitation and plasmon production, as shown below. Lundquist<sup>5</sup> has suggested that the electron-electron interaction can result in a new type of excitation called a plasmaron, a coupled hole-plasmon mode. This type of mode would influence the XPS loss spectra; however, there is no ex-

perimental evidence that the mode exists.

(a) *Intrinsic plasmon production.*—The production of an intrinsic plasmon accompanying photoexcitation of a conduction-band electron can be thought of as a two-step process: (1) An electron is photoexcited, and (2) a second electron creates a plasmon (or electron-hole pair) via its Coulomb interaction with the remaining conduction electrons and scatters into the hole left by the photoexcited electron. Both steps are virtual. In step one the photoexcited electron does not gain the full photon energy, while in step two the extra energy saved in step one is used to create a plasmon. The sequence of the two steps can be reversed: (1') An electron creates a plasmon and is scattered out of the Fermi sea, and (2') it is then photoexcited. In both cases the photoexcited electron contributes directly to the first loss peak in the XPS spectrum located at energy  $\hbar\omega_p$  below the no-loss peak. The probability that an electron is photoexcited to energy  $E$  without creation of a plasmon is

$$I_0(E, \hbar\omega_{\text{ph}}) = (2\pi/\hbar) \sum_{k_i k_f} f_{k_i} |\langle k_i | \tau | k_f \rangle|^2 \delta(E - \epsilon_{k_f}) \delta(E - \hbar\omega_{\text{ph}} - \epsilon_{k_i}), \quad (1)$$

where  $|k_i\rangle$ ,  $|k_f\rangle$  and  $\epsilon_{k_i}$ ,  $\epsilon_{k_f}$  are the initial- and final-state wave functions and energies of the photoexcited electron and  $\tau = (e/mc)\vec{A} \cdot \vec{P}$ . The probability of photoexciting an electron to energy  $E$  and simultaneously creating an electron-hole pair or plasmon by the processes described above is determined from time-dependent perturbation theory:

$$I_1(E, \hbar\omega_{\text{ph}}) = (2\pi/\hbar) \sum_{k_i k_f k'_q} f_{k_i} |\langle k_i + q | \tau | k_f \rangle|^2 f_{k'_q} (1 - f_{k'_q}) |\epsilon_{k_i + q} - \epsilon_{k_i} + \epsilon_{k'_q} - \epsilon_{k'_q} - i\Gamma|^{-2} \\ \times |\langle k_i, k'_q | V | k_i + q, k'_q - q \rangle|^2 \delta(E - \epsilon_{k_f}) \delta(E + \epsilon_{k'_q} - \epsilon_{k'_q} - \epsilon_{k_i} - \hbar\omega_{\text{ph}}). \quad (2)$$

Equation (2) describes photoexcitation of an electron from the state  $|k_i + q\rangle$  to  $|k_f\rangle$  and scattering of an electron from  $|k_i\rangle$  to  $|k_i + q\rangle$  by means of the excitation of a plasmon or electron-hole pair with energy  $\epsilon_{k'_q} - \epsilon_{k'_q}$  and momentum  $q$  via the interaction  $V$ , the screened Coulomb interaction<sup>6</sup>; the exchange interaction is neglected because I am primarily interested in plasmon excitations<sup>6</sup>; the exchange interaction modifies the electron-hole pair production, i.e., the broadening and tailing of the parent (no-loss) XPS spectra. In Eq. (2),  $\Gamma$  is the lifetime of the intermediate state. Equation (2) is consistent with an effective Hamiltonian derived from Bohm-Pines theory by earlier workers<sup>7</sup> to study the contribution to the optical conductivity,  $\sigma(\omega)$ , due to the simultaneous creation of a plasmon and an intraband electron-hole pair. This mechanism can result in a peak in  $\sigma(\omega)$  at an energy  $\hbar\omega_p$  above the Fermi energy.

An alternative derivation of Eq. (2) along the following lines provides additional insight into the mechanism of intrinsic plasmon production. The probability of photoexciting an electron from the state  $k_i$  to  $k_f$  depends on  $\langle \phi_i | \tau | \phi_f \rangle$  where  $\phi_i$  and  $\phi_f$  are the Slater determinants describing the ground state and the final state in which there is an electron in  $k_f$  and a hole in  $k_i$ . Electron correlations caused by the electron-electron interaction are taken into account by including the mixing of  $\phi_i$  and  $\phi_f$  with other states:

$$\Phi_j = \phi_j + \sum_{st, uv} (\epsilon_s + \epsilon_t - \epsilon_u - \epsilon_v)^{-1} \langle st | V | uv \rangle \phi_j(st | uv),$$

where  $j = i$  or  $f$  refers to the system wave function before or after photoexcitation and  $s, t$  are one-electron states of  $\phi_j$  while  $u, v$  are states not contained in  $\phi_j$ .  $\phi_j(st | uv)$  is the determinant  $\phi_j$  with the

states  $s, t$  replaced by  $u, v$ . The term in  $\langle \Phi_i | \tau | \Phi_f \rangle$  that is independent of  $V$  gives rise to  $I_0$  of Eq. (1) while the terms that are linear in  $V$  yield  $I_1$ , of Eq. (2). The summand in Eq. (2) corresponds to the terms  $s = k_i, t = k', u = k_i + q, v = k' - q$  in  $\Phi_i$  and  $s = k_i + q, t = k' - q, u = k_i, v = k'$  in  $\Phi_f$ . Consequently correlation effects (or configuration mixing) in both the initial and final states are responsible for the simultaneous processes of photoexcitation and electron-hole pair or plasmon excitation.

Equation (2) may be put in the form<sup>8</sup>

$$I_1(E, \hbar\omega_{\text{ph}}) = \int_0^\infty d(\hbar\omega) I_0(E, \hbar\omega_{\text{ph}} - \hbar\omega) \beta(E, \hbar\omega), \quad (3a)$$

$$\beta(E, \hbar\omega) = (1/\pi) \sum_q v_q |\Delta E|^{-2} \text{Im}[1/\epsilon(q, \omega)], \quad (3b)$$

$$\Delta E = \hbar\omega + \epsilon_{k_i+q} - \epsilon_{k_i} - i\Gamma, \quad (3c)$$

where  $v_q = (4\pi e^2/q^2\Omega)$ ,  $k_i$  is the momentum of the final hole state determined from  $\epsilon_{k_i} = E + \hbar\omega - \hbar\omega_{\text{ph}}$ , and  $\epsilon(q, \omega)$  is the dielectric function of the metal. If  $\Delta E$  is approximated by  $\hbar\omega$  in Eq. (3b) then Eq. (3) is identical to the perturbation-theory result for the core case if the core potential is described by the point-ion model rather than a pseudopotential. Just as in the core case there is an interference between the intrinsic process and the extrinsic one in which an electron is photoexcited in an energy-conserving transition and subsequently loses energy via creation of a plasmon or electron-hole pair. This interference results in the replacement of  $|\Delta E|^{-2}$  in Eq. (3b) by<sup>8</sup>

$$|\Delta E|^{-2} [1 + 2(\hbar\omega + \epsilon_{k_i+q} - \epsilon_{k_i})(\hbar\omega + \epsilon_{k_f} - \epsilon_{k_f-q})^{-1}],$$

where  $k_f$  is determined from  $(\hbar^2/2m)k_f^2 = E$ .

The quantity  $\beta$  in Eq. (3) can be evaluated analytically if it is assumed that the only excitation modes of the metal are dispersionless plasmons. This implies that  $\text{Im}[1/\epsilon(q, \omega)] = (\pi/2)\omega_p\delta(\omega - \omega_p)$  for  $q < q_c$ , where  $q_c$  is the critical momentum for plasmons. Use of this approximation in Eq. (3b) yields

$$\beta(E, \hbar\omega) = (e^2 q_c) / (\pi \hbar \omega_p) \Delta(E) \delta(\hbar\omega - \hbar\omega_p), \quad (4a)$$

where

$$\Delta(E) = \bar{\omega}_p / (8\bar{q}_c \bar{k}_i) \ln[(\bar{\omega}_p + \bar{q}_c^2 + 2\bar{k}_i \bar{q}_c) / (\bar{\omega}_p + \bar{q}_c^2 - 2\bar{k}_i \bar{q}_c)] \\ + (\bar{\omega}_p / 4\bar{q}_c) (\bar{\omega}_p - \bar{k}_i^2)^{-1/2} \{ \tan^{-1}[(\bar{q}_c + \bar{k}_i) / (\bar{\omega}_p - \bar{k}_i^2)^{1/2}] + \tan^{-1}[(\bar{q}_c - \bar{k}_i) / (\bar{\omega}_p - \bar{k}_i^2)^{1/2}] \} \quad (4b)$$

where  $\bar{\omega}_p = \hbar\omega_p/\epsilon_F$ ,  $\bar{q} = q/k_F$ , and  $k_F$  and  $\epsilon_F$  are the Fermi momentum and  $\bar{q}_c \approx \bar{\omega}_p/2$ . For a value of the electron density such that  $r_s = 2$ ,  $0.82 < \Delta(E) < 1.08$ , and for  $r_s = 4$ ,  $0.78 \leq \Delta(E) \leq 0.97$ . In the core-level case (assuming a point-ion model),  $\Delta(E) = 1$ . In the one-mode model the contribution of the interference effect to  $\beta$  is very close to that obtained for the core case;  $\beta$  is reduced from the value given in Eq. (4) by roughly 53% and 22% for  $r_s = 2$  and  $r_s = 4$ , respectively.

(b) *Calculation of the conduction-band XPS loss spectra.*—The most direct experimental evidence for the creation of intrinsic plasmons in conduction-band XPS is to be found in the loss spectra. The differences between the predicted loss spectra for Mg and Na with and without the inclusion of intrinsic plasmons are quite dramatic and provide a clear test for the presence of intrinsic plasmons. The theory of the loss spectra for conduction-band XPS is based on a three-step model: (a) photoexcitation of electrons, (b) transport to the surface, and (c) escape through the surface. The details for the core-level case are

contained in Ref. 2 and the difference between the core case and the conduction-band case is that Eq. (1) of that reference which describes the energy distribution of photoexcited electrons in step (a) is replaced by  $I_0 + I_1$  given by Eqs. (1) and (3) of this Letter. The internal photoexcited-electron-energy distribution is thus described by (1) a high-energy peak given primarily by Eq. (1) but taken from experiment for the purposes of this calculation, and (2) a peak of similar shape displaced downward in energy by  $\hbar\omega_p$  and predicted by Eq. (3).

The input parameters for the calculation of the loss spectra of Mg and Na are the plasmon dispersion and broadening as a function of momentum which enter in the model dielectric function given in Eq. (2) of Ref. 2 and the mean free path for core-electron excitation. Values for these quantities are given in that paper. Because  $\beta(E, \hbar\omega)$  of Eq. (3) is fairly independent of  $E$ , I have carried out the calculations neglecting the  $E$  dependence; this introduces a maximum error

of 4% in the calculated loss spectra. Just as in the core-level case the no-loss peak is taken from experiment, and the quantity  $\Gamma$  in Eq. (3) is adjusted so that the calculated spectrum predicted by Eq. (3) fits smoothly onto the no-loss peak at an energy  $\epsilon_F$  below the Fermi-level threshold.<sup>9</sup>

The results of the calculation are shown in Fig. 1. The calculations were carried out (a) including plasmon production, and (b) neglecting intrinsic plasmon production. The differences in the calculated spectra are striking. These differences appear in the higher loss peaks as well as the first loss peaks although multiple intrinsic plasmon production has been neglected. This is because electrons which are photoexcited with the simultaneous creation of an intrinsic plasmon can subsequently lose energy by exciting extrinsic plasmons and thus contribute to higher loss peaks. The experimental data of Höchst, Steiner, and Hüfner<sup>10</sup> are shown and the agreement between theory (a) (with intrinsic plasmons) and experiment is good. The difference between theory and experiment in the case of the multiple-loss peaks may be due to neglect of multiple-plasmon production in the theory. Just as in the core case, inclusion of the interference effect would reduce

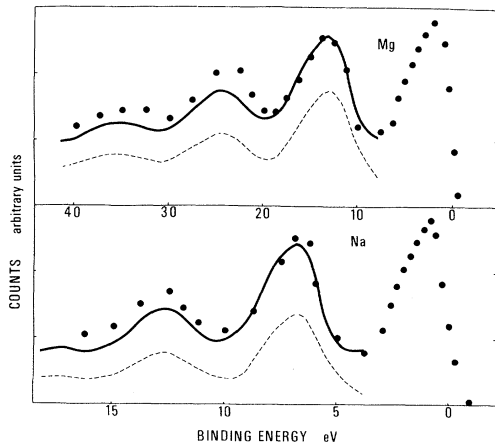


FIG. 1. Comparison of theory and experiment for the XPS valence-band loss spectra of Mg and Na. The dots represent experiment. The solid line is the complete theory and the dashed line is the theory without intrinsic plasmons and intrinsic electron-hole pairs. The no-loss peaks are taken from experiment and serve as input data for the calculations of the loss spectra.

the calculated loss spectrum (a) by roughly 10% for Mg and Na.

In conclusion, intrinsic plasmons are produced in XPS experiments on the conduction bands of nearly-free-electron metals and their contribution to the XPS loss spectra is remarkably close to that found in the core-level case despite the fact that they are produced by different mechanisms. In the core-level case the hole potential created by a photoexcited electron produces intrinsic plasmons while in the conduction-band case it is electron correlations that are crucial.

I am indebted to Dr. Paul Citrin for helping to interest me in the problem and for continuing discussions and encouragement during the course of the work. At the time when it became clear that there was an anomaly in the experimental XPS loss data, Dr. Citrin, with tremendous insight, predicted that the anomaly was due to intrinsic plasmons created by conduction-band correlations and this view is confirmed by the present theory and calculations.

<sup>1</sup>B. I. Lundqvist, Phys. Kondens. Mater. **9**, 236 (1969).

<sup>2</sup>David R. Penn, Phys. Rev. Lett. **38**, 1429 (1977).

<sup>3</sup>D. C. Langreth, Phys. Rev. B **1**, 471 (1970).

<sup>4</sup>P. Minnhagen, Phys. Lett. **56A**, 327 (1976).

<sup>5</sup>B. I. Lundqvist, Phys. Kondens. Mater. **6**, 193 (1967).

<sup>6</sup>D. Pines, *Elementary Excitations in Solids* (Benjamin, New York, 1963).

<sup>7</sup>N. Tzoar and A. Klein, Phys. Rev. **124**, 1297 (1961); N. Matsudaira, J. Phys. Soc. Jpn. **17**, 1563 (1962); R. J. Esposito, L. Muldower, and Philip E. Bloomfield, Phys. Rev. **168**, 744 (1968).

<sup>8</sup>David R. Penn, to be published.

<sup>9</sup>I find  $\Gamma = 2.2$  eV and  $\Gamma = 1.0$  eV for Mg and Na, respectively. These values of  $\Gamma$  are not of direct physical significance because the exchange term has been neglected in Eq. (3b). This is a good approximation for determining most of the loss spectra; however, it is not valid for small energy losses which contribute to the portion of the loss spectra at energies near  $\epsilon_F$  below the Fermi energy where  $\Gamma$  is determined. The value of  $\Gamma$  has virtually no effect on the main portion of the loss structure and only the dip between the no-loss and first loss peaks is sensitive to it.

<sup>10</sup>H. Höchst, P. Steiner, and S. Hüfner, J. Phys. F **7**, L309 (1977).